J. Electrical Systems 20-10s (2024): 7791-7810

[1] Ali Othman Mohammed [1],

Farzaneh Rahmani[2],

Shoorangiz Shams Shamsabad Farahani[3]

Ali Hassanein Alwaily[4],

Seyed Mohsen Saneii[5],

Alireza Izadi[6],

Mohammad Arabian[7],

Roohollah Barzamini[7,8,*]

A new Solar-IoT Based Method for Mushroom Cultivation

Journal of Electrical Systems

Abstract: - Although, Mushroom cultivation is a growing industry for recent years, but maintaining proper conditions in mushroom farms may be challenging, especially for small-scale farmers without accessibility to modern controller systems. In this paper, a new IoT-based approach based on Blynk platform for mushroom cultivation is presented. The Blynk dashboard includes gauges for monitoring humidity and temperature in real time, as well as sliders for controlling the environment situations. The sliders are connected to relays which are powered by a solar power system. This mechanism making it a proper option for using in a remote locations without access to main grid, also the low cost of the system makes it an affordable option for small-scale farmers. For improving the identification characteristic, a hybrid method consists of differential evolution algorithm and wavelet transform is used. The model is a classification model trained on a dataset of healthy and diseased mushrooms, which can determine the real-time conditions of mushrooms. For practical applications, reducing the number of extracted features and minimizing redundancy features have great importance. In the proposed method, features are extracted from the original data by applying differential evolution algorithm. Then these features were evaluated by methods such as logistic regression, k-nearest neighborhood and decision tree. It was found that among the specified features, the first two features covered more than 89% of the variance of the entire set. Then the wavelet transform method is applied to get final identifications. Finally, by reducing the number of features to 2, a considerable amount of calculations is reduced and only about 4% of the accuracy provided for the estimated results is reduced.

Keywords: Blynk platform; classification algorithms; IoT-solar system; Mushroom cultivation.

[1] [1]*Department of Electrical Engineering, Islamic Azad University Tehran Central Branch, Tehran, Iran*

Alialabidy38@gmail.com

[2]*Department of Information Technology Management, Islamic Azad University, South Tehran Branch, Tehran, Iran*

rahmani.f.it@gmail.com

[3]*Department of Electrical Engineering, Islamshahr branch, Islamic Azad University, Islamshahr, Iran*

shams@iiau.ac.ir

[4]*Kut Technical Institute, Middle Technical University, Baghdad, Iraq*

alihussainhadi@mtu.edu.iq

[5]*Business School, University of Roehampton, SW15 5PH, London, United Kingdom*

mohsen.saneii@gmail.com

[6]*Department of Electrical Engineering Islamic Azad University, Tehran Central Branch, Tehran, Iran Ali.izadi.eng@iauctb.ac.ir*

[7]*Department of Electrical Engineering, Islamic Azad University, Tehran Central Branch Tehran, Iran*

m.arabian.eng@ iauctb.ac.ir

[8]*Department of Engineering, City University of London, London, United Kingdom*

*r.barzamini.eng@iauctb.ac.ir, roohollah.barzamini@city.ac.uk**

*Alialabidy38@gmail.com; rahmani.f.it@gmail.com; shams@iiau.ac.ir; alihussainhadi@mtu.edu.iq; mohsen.saneii@gmail.com; Ali.izadi.eng@iauctb.ac.ir ; m.arabian.eng@ iauctb.ac.i ; r.barzamini.eng@iauctb.ac.ir, roohollah.barzamini@city.ac.uk**

I. Introduction

Smart agriculture emerges various technologies such as the Internet of Things (IoT), artificial intelligence (AI), data analytics, robotics, and remote sensing which enable farmers to make proper decisions based on real-time data for improving their crops while minimizing resource wastage [1]. In other side, with a growing world population and changing climatic conditions, traditional farming methods cannot meet

the increasing demand for food while ensuring environmental sustainability. So, smart agriculture addresses these challenges by providing farmers with data-driven insights and automation capabilities, enabling them to optimize resource utilization, reduce environmental impact, and improve crop quality [2]. By deploying sensors throughout the farm, smart agriculture systems can monitor key environmental parameters such as temperature, humidity, soil moisture, and nutrient levels. For example, by monitoring soil moisture levels using IoT-based sensors, the water can be applied only when necessary, causes reducing water consumption and minimizing the risk of over-irrigation, which can lead to waterlogging and nutrient leaching [3]. Also by analyzing weather patterns, soil conditions, and historical yield data, farmers can make informed decisions about the choice of crops, planting schedules, and optimal cultivation practices to maximize yield and minimize losses [4]. Moreover, by implementing precision farming techniques, such as variable rate application and targeted spraying, farmers can limit agrochemical use, reducing environmental contamination and improving ecosystem health [5]. In addition to these benefits, smart agriculture offers significant potential for increasing food production in a sustainable manner.

Traditional mushroom farms rely on manual monitoring and control, leading to inefficiencies, inconsistencies, and increased labor costs. Therefore, there is a need for an automated and sustainable solution that leverages IoT technology and renewable energy sources to enhance the efficiency and productivity of mushroom farms while reducing their environmental impact. Previous studies have used various methods to classify images based on spectral, structural, and textural features, but none of them have considered the impact of humidity and temperature on the accuracy of the approaches. Also, with producing the huge amount of data, identification and processing will be more complex and time consuming. Therefore, in this study the effect of humidity and temperature variations on the sensors performances are studied.

In this paper, two different sensors (Sensirion and DHT22) are used. Then, differential evolution algorithm (DEA) has been applied to the dataset to extract the features that are not correlated with each other. By applying DEA on the data set, the matrix of eigenvectors is obtained which significantly reduces the computation time and complexity space. Then, different classification methods such as logistic regression (LR), k-nearest neighbor (KNN) and decision tree (DT) are applied on the obtained features. These classifiers are chosen because they have a simple structure and their results can help improve the accuracy of detecting different characteristing of mushrooms. The results of other studies in this field demonstrate the superiority of neural networks over other state of the art methods in this field [42-44]. For performance evaluation of these methods, criterion such as ROC and F-1 score are used. For extracting the optimal amount of features, wavelet transform method is applied. The main contributions of this paper are as follows:

- Combinatining DEA with WT to extract effective features of mushroom cultivation.
- Defining multi-objective function, which researches for minimization classification error, the number of features and redundancy features simultaneously.

Nomenclature

Parameters

g : generation number

i : Individual index

j : Variable index

$x_j^{g,i}$: Variable j of individual I in generation g

u : trail vector

r : Random number

r_0 : Random number

CR : Crossover rate

c : Learning factor

S_{CR} : Set of indices

$|S_{CR}|$: Cordinality of set

r_3 : Random selected individual

r_4 : Random selected individual

F^i : Scaling factor

c : Learning factor

S_F : Set of individuals

$x_0, \dots, x_{N_F-1}$: Feature weight

x_{N_F} : Feature no.

D_i^a : Actual value

D_i^m : Measured value

$\overline{D}_i$: Mean value

J_2 : Fitness value of feature no.

N_f : No. of features in the subset

N_f^{th} : Max. no. of allowed features

II. CULTIVATION CHARACTERISTICS

Button mushrooms (Agaricus bisporus) are one of the most widely cultivated and consumed mushroom species worldwide. They have a mild flavor and a versatile culinary profile, making them popular in various dishes (Fig. 1). Let's discuss the cultivation aspects of button mushrooms, including substrate preparation, spawn inoculation, growing conditions, and harvesting.

- Substrate Preparation: Button mushrooms are typically cultivated on a substrate composed of composted materials. Common ingredients include wheat straw, horse or poultry manure, gypsum, and supplements like cottonseed meal or soybean meal. The composting process involves several stages of composting, pasteurization, and conditioning to create a suitable environment for mushroom growth [6]. Detailed substrate preparation techniques can be found in various cultivation guides [7 ,8].
- Spawn Inoculation: After the composting process, spawn is introduced into the substrate. Spawn refers to a mixture of mushroom mycelium and a carrier material (e.g., grain or sawdust). Spawn inoculation can be done by mixing the spawn with the compost or by placing spawn-infused grains on the surface of the compost [6].
- Growing Conditions: Button mushrooms require specific environmental conditions to initiate fruiting. These conditions include temperature, humidity, light, and fresh air exchange.
- Harvesting: Button mushrooms are typically harvested when the caps are fully expanded but before the veil beneath the cap breaks. Harvesting is usually done by twisting the mushrooms gently to separate them from the substrate. Once harvested, the mushrooms should be stored at a cool temperature to maintain freshness [8].

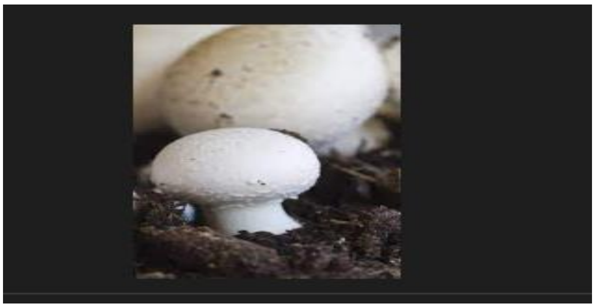

Fig. 1. Sample of button mushroom

A. Humidity Control

Humidity plays a crucial role in mushroom cultivation as it directly affects the growth, development, and overall yield of the mushrooms. Maintaining the appropriate humidity levels is essential to create an optimal environment for mushroom growth. Some of the the most advantages of Humidity Control in mushroom cultivation are optimal mycelium growth, water absorption, prevents drying out, disease prevention and uniform mushroom development.

B. Temperature control

Mushroom cultivation requires specific temperature ranges to ensure successful growth and development. The optimal temperature for mushroom cultivation varies depending on the species of mushroom being grown. Different species have different temperature requirements, and providing the appropriate temperature range is crucial for achieving optimal yields. Additionally, some mushroom species have different temperature requirements during different stages of growth, such as spawn run, primordia formation, and fruiting (Table 1) [9].

C. Cultivation Aspects

In mushroom cultivation, there are several important aspects to consider in order to create proper growing conditions to maximize productivity. Some of key engineering aspects related to mushroom cultivation are environmental control, substrate preparation, sterilization and sanitation, lighting systems, automation and monitoring, and energy efficiency. These aspects are vital for the commercial-scale cultivation of mushrooms, allowing for efficient and controlled production.

Table 1. Temperature ranges for different stages

Mushroom Species	Spawn Run	Primordia Formation	Fruiting
Button Mushrooms	21-26°C (70-78°F)	18-21°C (64-70°F)	12-18°C (54-64°F)
Oyster Mushrooms	24-28°C (75-82°F)	10-18°C (50-64°F)	10-20°C (50-68°F)
Shiitake Mushrooms	24-28°C (75-82°F)	10-16°C (50-60°F)	10-24°C (50-75°F)
Enoki Mushrooms	10-12°C (50-54°F)	5-12°C (41-54°F)	5-12°C (41-54°F)

III. LITERATURE REVIEW

A. Cultivation process

Writers of [10] investigated the effect of different light conditions on the growth and nutrient content of shiitake mushrooms (Lentinula edodes). The found that mushrooms grown under full-spectrum LED lights exhibited higher biomass accumulation compared to those grown under fluorescent lights. In [11] the impact of various cultivation substrates on the medicinal properties of reishi mushrooms (Ganoderma lucidum) are studied. The results showed that substrates supplemented with herbal extracts significantly enhanced the bioactive compound content and antioxidant activity of the mushrooms, highlighting the potential for targeted cultivation techniques to boost medicinal properties. In [12] the feasibility of utilizing agricultural waste, such as wheat straw and corn cobs, as substrates for oyster mushroom cultivation are evaluated. The study demonstrated that these low-cost substrates supported successful mushroom growth and yielded comparable results to traditional substrates, offering a sustainable and economically viable alternative.

B. IoT-Blynk technology

Writers of [13] presents a study on the implementation of IoT-Blynk (a popular Internet of Things (IoT) platform) for enhancing agricultural efficiency. The system leverages IoT sensors, actuators, and the Blynk mobile application to create a smart farming environment. The integration of IoT-Blynk enables real-time data collection, remote monitoring, and automated control of critical farming parameters. The experimental results demonstrate improved crop yield, resource optimization, and reduced manual efforts.

In [14] wireless sensors are used to collect data on soil moisture, temperature, humidity, and light intensity. This information is then transmitted to the Blynk mobile application, allowing farmers to remotely monitor the field conditions and make informed decisions. Moreover, the system employs actuators to automate irrigation and adjust environmental factors based on preset thresholds. The experimental evaluation of the system demonstrates its effectiveness in optimizing resource usage, reducing water consumption, and improving crop yield.

C. Artificial Intelligence

Artificial intelligence (AI) can be used to analyze large quantities of data collected from sensors and other IoT-related devices, providing valuable insights for decision-making to improve environmental conditions. Evolution-based algorithms begin with an initial population and utilize operators such as selection, mutation, crossover, and elitism to generate subsequent generations. Notable algorithms in this category include the genetic algorithm (GA) [15], evolution strategy [16], and differential evolution [17]. Population-based algorithms are based on movement of particles. Some optimization algorithms belonging to this category include the particle swarm optimization (PSO) algorithm [18], ant colony optimization (ACO) [19], and bee swarm optimization [20]. These algorithms utilize the behavior and interactions observed in particle or bird swarms to solve optimization problems.

D. Feature selection

With advancements in technology, it is possible to extract features from information that capture various details. These features represent different characteristics in the given situation. However, solving huge problems using traditional mathematical approaches is often impractical or time-consuming. So, meta-heuristic algorithms can provide effective solutions, taking into account large datasets and various constraints. In [21], a modified genetic algorithm (GA) is employed for feature extraction, demonstrating a robust evolutionary structure and delivering acceptable performance. The objective function incorporates a penalty coefficient to prevent violations and extract the desired feature values.

In [22], a modified particle swarm optimization (PSO) algorithm, known as competitive swarm optimizer, is utilized to select a subset of features that accurately represents the dataset. This approach handles a large set of diverse features and produces continuous values, which can be further used in subsequent evaluations. In [23], the genetic algorithm (GA) was employed to sort the features obtained from other filtering methods. Additionally, in [24], the gray wolf algorithm was utilized for feature extraction. Through the examination of various studies and articles, it was observed that in many cases, only one objective, typically classification accuracy, was investigated, while other goals such as the number of features were not taken into account during the modeling process. A summarized review of these approaches can be found in Table (2-3).

IV. HARDWARE REQUIREMENTS

This section contains the main components required to observe and control the environmental conditions. This structure consists of sensors, micro-controller, relays, solar panels, inverter and batteries.

A. DHT22 sensor

The DHT22 sensor, also known as the AM2302, is a widely used temperature and humidity sensor in IoT applications, including smart agriculture systems.

Table 2. Comparison of different feature selection algorithms

Ref.	Name of Classifier	Evaluation Metrics
[25]	Bayesian regularization artificial neural network (BRANN) method	Mean, median, and standard deviation of fitness function values
[26]	Improved SVM with Chaos maps + Quadratic programming	Accuracy of feature classification
[27]	Fuzzy logic classifier	Accuracy of feature classification
[28]	K-nearest neighbor (KNN)	Best, Worst, Avg values
[29]	Optimum forest (OF)	Accuracy of feature classification
[30]	Random forest (RF)	Classification accuracy + Matthew's correlation coefficient + Area under curve (AUC)
[31]	K-nearest neighbor (KNN)	Selected no. of features + Classification accuracy
[32]	Supprot vector machine (SVM)	F-measure + Avg no. of selected features

Accurate and reliable measurements, making it an ideal choice for monitoring the environmental conditions in a smart mushroom farm based on solar-IoT technology. The DHT22 sensor utilizes a capacitive humidity sensing element and a digital temperature sensor to provide precise readings. Its key features, such as a wide measurement range (-40°C to 80°C for temperature and 0% to 100% for humidity) and a high accuracy level (±0.5°C for temperature and ±2% for humidity), ensure the collection of reliable data for effective control and monitoring [33] (Fig. 2).It should be noted that the family of DHT22 sensors are among the cheapest sensors in the electronic devices' market. These sensors consist of 3 main parts such as a thermistor, a humidity-sensitive part, and an analog-to-digital signal conversion circuit. In order to calibrate their performance, usually the values measured by these sensors are compared with the results obtained from sensors that have a high level quality. For this purpose, in this project, the sensors of the SHT group are used, which are products of the Sensirion company.

Fig. 2. A sample of DHT22 sensor [33]

These sensors have very high performance quality and accuracy, and due to their high accuracy, stable performance and good quality, this group of sensors is usually used in operating room equipments and sensitive medical devices. One of the unique features of this group of sensors is their digital calibration, which means that there is no need for re-calibration and they do not lose their original accuracy and quality under natural conditions. Therefore, they can be a suitable reference for evaluating the accuracy of sensors that have a lower cost and quality.

B. Esp32 Microcontroller

The ESP32 is a powerful microcontroller that has gained significant popularity in IoT-based applications due to its advanced features and capabilities. The ESP32 microcontroller is based on the Xtensa LX6 CPU architecture and operates at clock frequencies of up to 240 MHz. It features dual-core processing, allowing for the simultaneous execution of multiple tasks and efficient multitasking capabilities. This makes it well-suited for handling the complex tasks required in a smart mushroom farm, such as sensor data processing, control algorithms, and communication with external devices [33]. One of the standout features of the ESP32 is its built-in Wi-Fi and Bluetooth connectivity. This connectivity is crucial for remote monitoring and control of the smart mushroom farm, as well as for data transmission to cloud platforms for further analysis [34]. The ESP32 also features a rich set of peripherals, including multiple UART, SPI, I2C, and GPIO interfaces, allowing for seamless integration with various sensors, actuators, and other external devices. These interfaces enable the connection of temperature and humidity sensors, relays for actuator control, display modules for user interfaces, and other components required in the smart mushroom farm system [35]. The ESP32's low-power operation, cryptographic hardware support, and vibrant developer community further enhance its suitability for building sustainable and secure IoT applications.

C. Relays

Relays serve as switches that control various components in the farm, enabling automated control based on sensor readings and user-defined settings. Indeed, relays act as intermediary devices between the microcontroller and the actuators, allowing the microcontroller to control high-power devices without directly handling the load. The primary usage of these devices are ventilation control, heating regulation, misting system, and lighting. Additionally, the ability to integrate relay-based control with the IoT platform (such as Blynk) allows remote monitoring and control of the farm, providing convenience and flexibility [36].

D. Solar panels

Photovoltaic panels (PV) harness sunlight and convert it into electricity, providing a renewable and sustainable energy source. For better applications of solar panels, several considerations such as PV capacity, energy efficiency, orientation and tilt, and maintenance and durability should be taken into account.

E. Inverters

They convert the direct current (DC) power generated by the solar panels into alternating current (AC) power that can be utilized by the farm's components. They are responsible for injecting power for sensors, microcontrollers, communication modules, actuators, and other electronic components [37]. Also they provide control mechanisms for regulating and maintaining the required voltage and frequency levels. In terms of energy efficiency, solar inverters optimize the power output from the solar panels and employ maximum power point tracking (MPPT) algorithms to extract optimum power under different environmental conditions.

F. Batteries

Storage batteries enable the storage of excess solar energy generated during peak sunlight hours for later use, ensuring a continuous power supply even when sunlight is insufficient or unavailable. They have numerous benefits, including energy independence, environmental friendliness, cost savings, and scalability.

V. RESEARCH METHODOLOGY

The traditional methods of mushroom cultivation often rely on manual monitoring and control, leading to inconsistent growth conditions and increased labor requirements. In order to address these challenges and improve the efficiency of mushroom cultivation, the integration of IoT and solar technology has emerged as a promising solution.

A. Hardware Components

In order to connect the DHT22 temperature and humidity sensor, ESP32 microcontroller, and two relays (for controlling a fog machine and an air conditioner) as shown in the Fig. (3), the following steps are done:

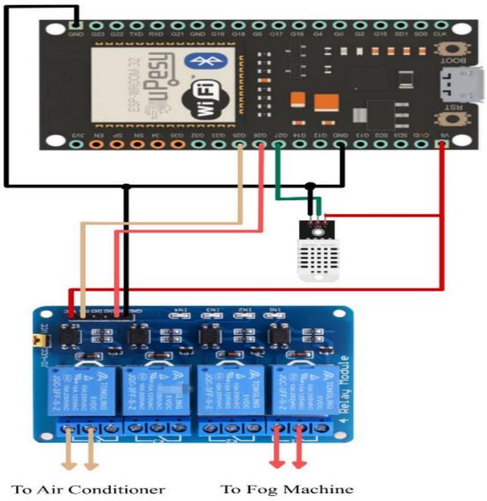

Fig. 3. Circuit diagram for controlling of humidity/temperature

1- Gather the necessary components: DHT22 sensor, ESP32 microcontroller, two relays, fog machine, air conditioner, jumper wires, and a breadboard.

2- Connecting the power supply to components:

- 3.3V pin of the ESP32 to the positive rail
- GND pin of the ESP32 to the negative rail.
- VCC pin of the DHT22 sensor to the positive rail.
- GND pin of the DHT22 sensor to the negative rail.

3- Connect the DHT22 sensor to the ESP32:

- Data pin of DHT22 to any digital pin of the ESP32.
- VCC pin of the DHT22 sensor to the 3.3V rail.
- GND pin of the DHT22 sensor to the GND rail.

4- Connect the relays to the ESP32:

- Control pin of the first relay to GPIO25 of the ESP32.
- Control pin of the second relay to GPIO26 of the ESP32.
- VCC pin of both relays to the 3.3V rail on the breadboard.
- GND pin of both relays to GND rail on the breadboard.

5- Connect the fog machine and air conditioner to the relays
6- Finally, provide power to the ESP32 and the external devices (fog machine and air conditioner)

To determine the requirements for a solar power system to support the mentioned appliances, there is need to consider the power consumption, available sunlight, battery capacity, and inverter size according to Fig. (4). For each day, average sunlight hours are considered about 10 hours and required solar panel capacity for supplies this demand is equal to 27296 Wh/ 10 hours = 3000 Watt. Considering that each panel has 600 Watt capacity and 1500 Watt is considered for power losses, then 75 solar panel are need for this project. For storage system, one day is determined for backup and according to rated voltage (12 V), total capacity of storage system is 27296

Wh/12 V = 227467 Ah, so 12 batteries are needed. The rated power of inverter is equal to 4716 Watt (Fogger + Air conditioner + Lights = 400*2 + 3516 + 300).

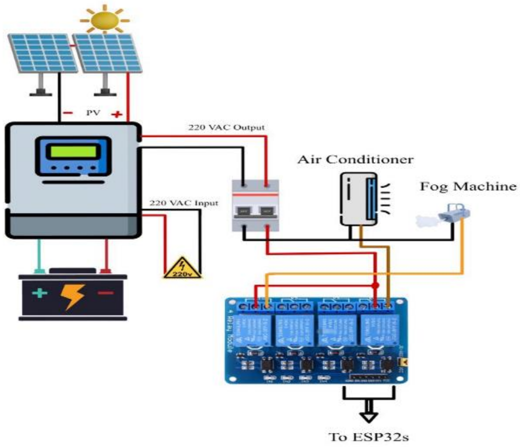

Fig. 4. Schematic of solar power system

B. Software Components

The software package includes the Blynk application and Web dashboard. Blynk is a popular IoT platform that allows users to create their custom applications for controlling and monitoring their connected devices. Blynk provides an easy-to-use interface and offers a range of widgets that can be easily configured and customized to meet specific needs.

C. Classification model

Classification methods are used to analyze the status of mushrooms for realizing any diseases on the infected plants and sending alerts to farmers to take emergency actions. This was done by a dataset of images. In this regard, feature selection can be used to improve the speed of convergence. This leads to a less complex prediction model. So, the choice of the appropriate feature is a crucial element for effective estimating since it will enhance knowledge of the estimated model and produce better outcomes. To select a set of related and efficient features, a two-step approach is presented:

1- Using the acquired data, create the initial set of candidate variables by taking into account all variables.

2- Using the feature selection approach, choose a subset of these variables.

D. Differential Evolution algorithm

The Differential Evolution (DE) algorithm is a global computer search algorithm introduced in 1995 by an American research team and was initially introduced to solve Chebyshev polynomials [38]. The important features of DE are simplicity, being efficient, easy to understand and programming, reliable operating results, high stability and fast convergence.

In the evolution phase, two individuals are selected from the population of the previous generation, and through the crossover operation, two children are generated for the next generation. The crossover operator has a lot of different methods and for this project, Equ. (1) is used. The function presented in Equ. (2) is used for generation a random value based on the gaussian distribution function, which output is in the range of [0.0,1.0]. The average value of the mentioned function is updated in each generation according to Equ. (3). After generating a chain of variables both for the current generation and for the next generation, the mutation operator is used to increase the search probability of finding points outside the local range. In the selection stage, since the implementation is based on the given weights, the more weight is applied to a feature, the more likely it is to be selected in the selection stage.

$$u_j^{g+1,i} = \begin{Bmatrix} x_j^{g,i} & if\ r \leq CR^i \\ x_j^{g,r_1} & if\ r_0 \leq 0.5 \\ x_j^{g,r_2} & o.w. \end{Bmatrix} \tag{1}$$

$$CR^i = Gauss(\mu_{CR}, 0.1) \tag{2}$$

$$\mu_{CR} = (1.0 - c) \times \mu_{CR} + c \times \frac{\sum_{i \in S_{CR}} CR^i}{|S_{CR}|} \tag{3}$$

In this situation, each gene is defined as Equ. (4). Then, to form a subset of features, the highest parameters that have been obtained for N_F are selected that have the highest weighting. To evaluate the variables in each generation, Equ. (5) is used and the scaling factor is also used according to Equ. (6). The Cauchy function can generate a random number by using the Cauchy distribution function and specifying the mean values and the corresponding standard deviation (Equ (7)) .

$$Gene\colon x_0, \dots, x_{N_F-1}, x_{N_F} \tag{4}$$

$$u_i^{g+1,i} = x_j^{g,i} + F^i \times \left(x_j^{g,r_3} - x_j^{g,r_4}\right) \tag{5}$$

$$F^i = Cauchy(\mu_F, 0.1) \tag{6}$$

$$\mu_F = (1.0 - c) \times \mu_F + c \times \frac{\sum_{i \in S_F} (F^i)^2}{\sum_{i \in S_F} F^i} \tag{7}$$

To perform the mutation operation, polynomial mutation is used in this project [39]. In this case, the mutation mechanism according to Equ. (8) and the mutation probability value according to Equ. (9) have been used in the modeling. In the evolving stage, Equ. (11) is used for each generation. The meaning of r is a uniform random number generated in the interval [0.0,1.0]. Equ. (12) is used to create mutations on the created children.

$$x_i^{g+1,i} = PM(u^{g+1}, pm) \tag{8}$$

$$pm = \frac{1}{nDim} \tag{9}$$

$$nDim = N_F + 1 \tag{10}$$

$$u_j^{g+1,i} = \begin{Bmatrix} x_j^{g,r_5} & if\ r \leq CR_B^i \\ x_j^{g,i} & o.w. \end{Bmatrix} \tag{11}$$

$$x_j^{g+1,i} = \begin{Bmatrix} 1 - u_j^{g+1,i} & if\ r \leq pm \\ u_j^{g+1,i} & o.w. \end{Bmatrix} \tag{12}$$

E. Wavelet Transform

The wavelet transform is a multi-scale signal analysis technique that builds on the concept of a fixed-resolution Fourier transform and is capable of performing high-quality signal analysis due to its multiple resolution characteristics. Additionally, it is the perfect instrument for processing and frequency analysis. This method divides the original image into four frequency domains: low-frequency level (LL) and high-frequency level LH, HL, and HH. LL has the most similarity among them to the original sub-image, which is referred to as subband approximation. The other three levels (LH, HL, HH) represent the image’s horizontal, vertical and diagonal details. In addition, the low-frequency subband can also be divided into four different subbands.

F.. Objective function

In this project, the differential evolution algorithm is used for extracting the effective features from original data and wavelet transform method will be used to improve the efficiency of the approach by reducing the number of features while keep the accuracy in the proper range. For this regard, the mean absolute percentage error (MAPE) is calculated. Equ. (13) is used to calculate the correlation between the obtained data and the real data [40]. The purpose of using this relationship is to measure the efficiency and performance of the sensors which used in the under study system. In order to determine the error for each sensor, mean absolute percentage error (MAPE) is calculated according to Equ. (14) [41].

$$R^2 = 1 - \frac{\sum_{i=1}^{n}(D_i^a - D_i^m)^2}{\sum_{i=1}^{n}(D_i - \bar{D}_i)} \tag{13}$$

$$MAPE = \frac{100}{n} - \sum_{i=1}^{n}\left|\frac{D_i^m - D_i^a}{D_i^a}\right| \tag{14}$$

Determining of feature numbers

This part is related to the no. of features obtained for each subset. The value of the function defined in this section is obtained by the Equ. (15). To determine the value of the objective function determined for the no. of features, constraints are introduced that limit their numbers. This limitation has 2 stages. In the first stage, the no. of features (N_f) is randomly determined from the range between $[1, N_F^{th}]$. In the second level, the values are set based on adding or subtracting different features to regulate cardinality values.

$$J_2 = \frac{N_f}{N_f^{th}} \tag{15}$$

Determining of feature redundancy

In this section, the correlation coefficient, known as Pearson coefficient, is used to measure the correlation value among the features, whose model is according to Equ. (16). The value of the fitness function for this part is also obtained through the Equ. (17). The flowchart of the proposed approach is shown in Fig. (5). This figure shows that the input image is first loaded into the system. Then, to speed up the feature selection operation, wavelet transformation (WT) is first used to obtain the efficient features. This significantly helps the speed of convergence.

$$r(F_\propto, F_\beta) = \left|\frac{\sum_{i=1}^{N_s}(F_\alpha(i) - \bar{F}_\alpha)(F_\beta(i) - \bar{F}_\beta)}{\sqrt{\sum_{i=1}^{N_s}(F_\alpha(i) - \bar{F}_\alpha)^2} \cdot \sqrt{\sum_{i=1}^{N_s}(F_\beta(i) - \bar{F}_\beta)^2}}\right| \tag{16}$$

$$f_R = \frac{1}{N_f(N_f - 1)/2}\sum r(F_\alpha, F_\beta) \tag{17}$$

VI. RESULTS ANALYSIS

A. Evaluation of Temperature Sensor Accuracy

In this project, the DHT22 sensor is used to measure humidity and temperature, because it has good performance accuracy and proper cost. Since it is necessary to ensure the accuracy of the measurements at the beginning of the operation, the values measured by the SHT31 sensor are used as reference values to confirm the calibration of the DHT22 sensor. To compare the temperature readings of the DHT22 and SHT31 sensors, data was collected simultaneously from both sensors. The temperature readings were recorded at regular intervals over a specific duration (Table 3).

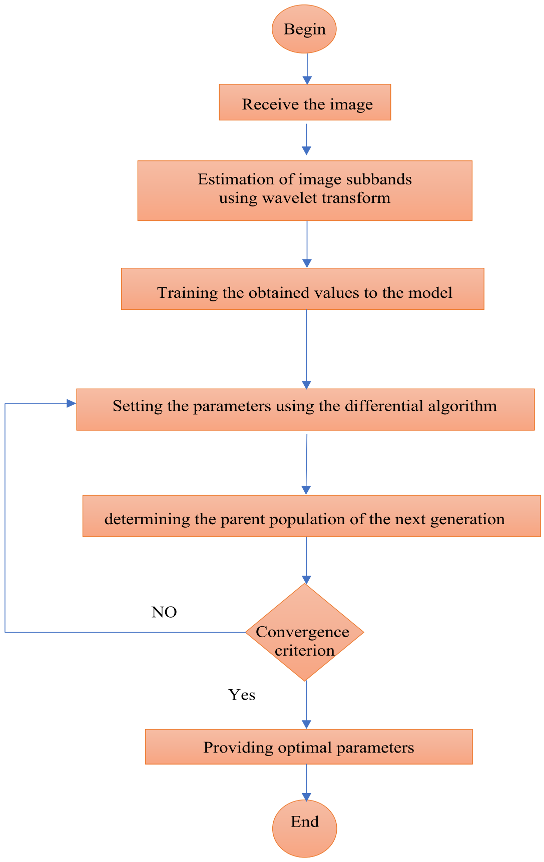

Fig. 5. Flowchart of proposed approach

In the "Temperature State" column, TP represents True Positive (DHT22 temperature within ±0.5°C of Sensirion temperature), FP represents False Positive (DHT22 temperature deviates by more than ±0.5°C), and FN represents False Negative (Sensirion temperature within ±0.5°C, but DHT22 temperature does not meet the criteria). According to Table 3, the amount of TP, FP and FN are equal to 10, 2 and 0, respectively. The accuracy of temperature readings is calculated as Equ. (18). So, this sensor can be used in the Mushroom farm in our farm.

$$\text{Accuracy} = \left(\frac{\text{TP}}{\text{TP} + \text{FP} + \text{FN}}\right) * 100\% = 83.33\% \qquad (18)$$

Table 3. Temperature Readings For DHT22 and SHT31

Reading No.	Sensirion Temp. (°C)	DHT22 Temp. (°C)	Temp. State
1	25	26	FP
2	25.2	25.9	TP
3	24.9	25.3	TP
4	25.3	25.8	TP
5	26.1	26.2	TP
6	25.2	25.7	TP

7	25.8	26.1	TP
8	25.3	25.9	TP
9	25.2	26	FP
10	25.5	25.8	TP
11	25.4	25.6	TP
12	25.1	25.7	TP

B. Evaluation of Humidity Sensor Accuracy

To compare the performance of DHT22 sensor for humidity measurement, the obtained measurements are presented in Table 4.

- TP (True Positive): Count the number of DHT22 humidity readings that fall within ±2% of the corresponding Sensirion humidity readings.
- FP (False Positive): Count the number of DHT22 humidity readings that deviate by more than ±2% from the corresponding Sensirion humidity readings.
- FN (False Negative): Count the number of Sensirion humidity readings that fall within ±2%, but the corresponding DHT22 humidity readings do not.

According to extracted results from Table 4, the accuracy for humidity readings is equal to Equ. (19).

$$\text{Accuracy} = \left(\frac{\text{TP}}{\text{TP} + \text{FP} + \text{FN}}\right) * 100\% = 91.67\% \qquad (19)$$

Table 4. Humidity Readings For DHT22 and SHT31

Reading No.	Sensirion Humidity	DHT22 Humidity	Humi. State
1	73	70	FP
2	72	71	TP
3	71	71	TP
4	70	69	TP
5	72	71	TP
6	73	71	TP
7	69	67	TP
8	70	68	TP
9	71	69	TP
10	68	66	TP
11	69	68	TP
12	72	71	TP

C. Dataset

In this project, data that include the appropriate level of moisture/temperature are needed to ensure the proper environment for mushroom growth. Also, special data on the appropriate levels of light, soil moisture, and acidity are required to produce proper output. The sample data which are used in this project are shown in Fig. (6).

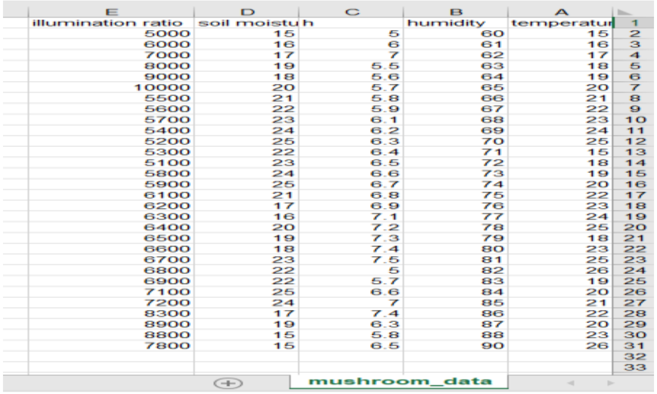

E	D	C	B	A	
illumination ratio	soil moistu	h	humidity	temperatur	1
5000	15	5	60	15	2
6000	16	6	61	16	3
7000	17	7	62	17	4
8000	19	5.5	63	18	5
9000	18	5.6	64	19	6
10000	20	5.7	65	20	7
5500	21	5.8	66	21	8
5600	22	5.9	67	22	9
5700	23	6.1	68	23	10
5400	24	6.2	69	24	11
5200	25	6.3	70	25	12
5300	22	6.4	71	15	13
5100	23	6.5	72	18	14
5800	24	6.6	73	19	15
5900	25	6.7	74	20	16
6100	21	6.8	75	22	17
6200	17	6.9	76	23	18
6300	16	7.1	77	24	19
6400	20	7.2	78	25	20
6500	19	7.3	79	18	21
6600	18	7.4	80	23	22
6700	23	7.5	81	25	23
6800	22	5	82	26	24
6900	22	5.7	83	19	25
7100	25	6.6	84	20	26
7200	24	7	85	21	27
8300	17	7.4	86	22	28
8900	19	6.3	87	20	29
8800	15	5.8	88	23	30
7800	15	6.5	90	26	31
					32
					33

Fig. 6. Sample of input data

D. DEA Results

In the first stage, the DEA approach has been applied to the dataset obtained from the evaluation of images. In this method, features are extracted which are called main features that are not correlated with each other. By applying DEA on the data set, the matrix of eigenvectors is obtained in the form of Equ. (20). In Equ. (21), the eigenvalues related to the data set are also stated. The percentage variance of each characteristic, which is also called "explained variance", is calculated based on Equ. (22) and the results obtained by it are presented in Equ. (23).

$$A = \begin{bmatrix} 0.448 & -0.116 & 0.005 & -0.111 & -0.611 & -0.100 & -0.624 \\ 0.443 & 0.137 & -0.101 & 0.495 & 0.0876 & -0.686 & 0.228 \\ 0.389 & -0.375 & 0.236 & -0.656 & 0.384 & -0.240 & 0.130 \\ 0.203 & 0.611 & -0.629 & -0.426 & 0.075 & 0.054 & 0.020 \\ 0.451 & -0.0877 & 0.037 & 0.056 & -0.392 & 0.471 & 0.640 \\ -0.056 & -0.667 & -0.731 & 0.109 & 0.057 & 0.023 & -0.002 \\ 0.451 & 0.034 & 0.044 & 0.340 & 0.555 & 0.487 & -0.364 \end{bmatrix} \quad (20)$$

$$\lambda = \begin{bmatrix} 0.4.838 \\ 0.1.455 \\ .0.630 \\ .0.057 \\ .0.022 \\ .0.006 \\ .0.001 \end{bmatrix} \quad (21)$$

$$V_j = \frac{\lambda_j}{\sum_{j=1}^{p} \lambda_j} \quad , \quad j = 1,2,\dots,p \quad (22)$$

$V_1 = .0.690$ (19) $V_3 = .0.090$ $V_4 = .0.008$ (23)

$V_5 = .0.003$ $V_6 = .0.001$ $V_7 = .0.000$

Scree plot and Pareto plot can be used to present the explained variance results. These are tools that measure the difference between the model data and the actual data set and present the results. This type of variance is obtained from the reduced features and not from the total features of the entire original data set. In these equations, λ_j indicates the eigenvalue and V_j indicates the variance value of the jth feature. As shown from the obtained results, the variance of the first characteristic is more than 69% ($V_1 = .0.690$) and the variance of the first two characteristics has a contribution of more than 89% ($V_1 + V_2 = 0.897$) of the total variance of the original data set. The obtained Scree plot and Pareto plot are shown in Fig. (7) and Fig. (8), respectively.

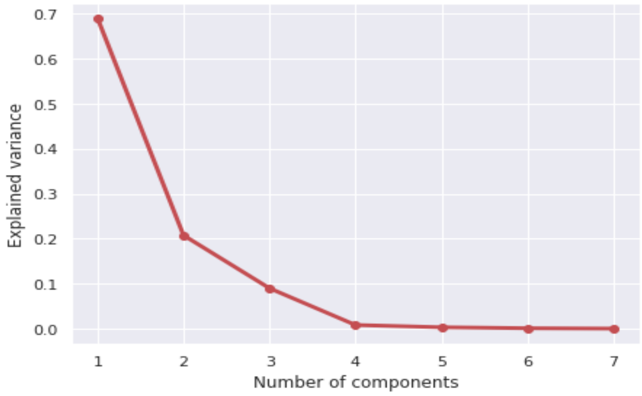

Fig. 7. Scree Plot

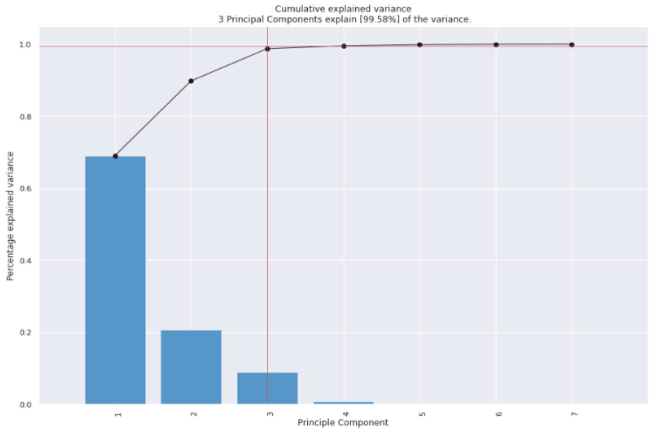

Fig. 8. Pareto Plot

As seen in Fig. (8), the knee point appears in the second characteristic, which shows that the dimensions of the characteristics can be reduced to r = 2. This significantly reduces the computation time and complexity space. According to the Pareto plot results, the first three features for more than 99.5% of the variance. In fact, each column represents the components of the related features. It should be noted that if the contribution of the feature is close to zero, this coefficient is ignored.

E. Classification Results before WT

In this section, the results obtained from applying different classification methods such as logistic regression (LR), k-nearest neighbor (KNN) and decision tree (DT) on the original data set are compared with each other. For this evaluation, there are many criteria such as confusion matrix (CM), decision boundary, prediction error and F-1 criterion. Among the 90 study samples, 81 samples were used for model design and parameter determination, and the rest were used for prediction accuracy analysis. Among the 81 samples selected for modeling, 70% of the data set was selected for training and the other 30% for testing. This comparison helps us to find the most suitable model with the highest accuracy among different techniques. Based on the obtained results, logistic regression (LR) has the best performance with an accuracy of 88.52%. After LR, Extra Tree (ET) and Random Forest (RF) classification are ranked second and third with 87.63% and 86.93% accuracy. In other words, if there are 1000 samples, LR methods are able to classify 885 samples correctly. For ET and RF classifiers, the estimated results are 876 and 869, respectively.

F. *Classification Results after WT*

In this section, the results of applying the WT method are analyzed. According to the results obtained in the previous sections, the first two characteristics account for more than 89% of the total explained variances. Therefore, the introduced approach is only applied to these two features. After applying WT, the best accuracy is extracted by KNN algorithm. The results obtained in these conditions are shown in Fig. (9). As can be seen in this figure, 212 out of 244 samples are correctly predicted. It means that the estimation accuracy after applying WT is more than 86%. If we compare the results extracted before and after applying WT, the error is around 0.4%. These results are actually a valid reason for using WT in this research project. In other words, by using the WT method, the division of features is reduced to 2, and the calculation error is less than 0.5%. If the results extracted before and after applying WT are compared, the error is around 0.4%. In other words, by using the WT method, the number of features is reduced and the calculation error is less than 0.5%. It can be seen from the results of Table 5 that the criteria of the adjusted LR model are better than the criteria of the basic model (before applying WT).

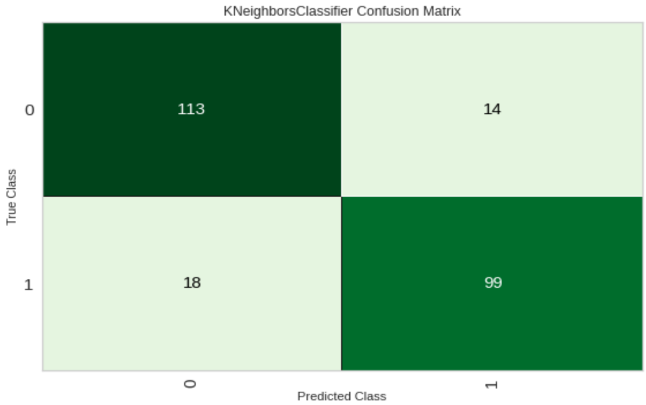

Fig. 9. Results after applying WT

Table 5. The results of applying classification models after WT

	Model	Accuracy	AUC	Recall	Prec.	F1	Kappa	MCC	TT (Sec)
knn	K Neighbors Classifier	0.8604	0.9060	0.8108	0.9032	0.8541	0.7211	0.7255	0.014
lr	Logistic Regression	0.8570	0.9206	0.8424	0.8748	0.8561	0.7139	0.7179	0.012
ridge	Ridge Classifier	0.8569	0.0000	0.7969	0.9102	0.8486	0.7142	0.7212	0.008
lda	Linear Discriminant Analysis	0.8569	0.9213	0.7969	0.9102	0.8486	0.7142	0.7212	0.012
lightgbm	Light Gradient Boosting Machine	0.8553	0.9056	0.8283	0.8792	0.8517	0.7107	0.7137	0.207
nb	Naive Bayes	0.8552	0.9199	0.7933	0.9089	0.8467	0.7107	0.7171	0.013
ada	Ada Boost Classifier	0.8517	0.9077	0.8145	0.8839	0.8465	0.7036	0.7076	0.079
qda	Quadratic Discriminant Analysis	0.8463	0.9112	0.7865	0.8994	0.8370	0.6930	0.7011	0.011
rf	Random Forest Classifier	0.8429	0.9069	0.8004	0.8800	0.8366	0.6859	0.6909	0.185
gbc	Gradient Boosting Classifier	0.8412	0.9094	0.8144	0.8657	0.8376	0.6824	0.6858	0.081
et	Extra Trees Classifier	0.8357	0.9171	0.8001	0.8651	0.8290	0.6716	0.6763	0.248
svm	SVM - Linear Kernel	0.8184	0.0000	0.8387	0.8202	0.8257	0.6367	0.6430	0.011
dt	Decision Tree Classifier	0.8007	0.8004	0.8107	0.8023	0.8039	0.6010	0.6052	0.011
dummy	Dummy Classifier	0.5035	0.5000	1.0000	0.5035	0.6698	0.0000	0.0000	0.013

VII. PERFORMANCE EVALUATION

A. *F-1 Score*

One of important criteria for performance evaluation is F1-score. This method uses the accuracy and recall of a classifier and then combines them with each other to create a criterion by considering the harmonic mean and the result is obtained by Equ. (24). This approach is commonly used to determine the best classifier among different methods. After applying all these methods and comparing the results extracted from the original data set, the logistic regression (LR) method obtained the best accuracy (more than 88.5%) among the other techniques. After LR, the second and third place is given to ET and RF classifications with 87.63% and 86.93% accuracy, respectively.

$$F1 - score = 2 \times \frac{precision \times recall}{precision + recall} \tag{24}$$

B. Receiver Operating Characteristic

One of the common criteria for evaluating the performance of classification methods is the receiver operating characteristic (ROC) metric. In this criterion, true positive values are located on the vertical axis and false positive values are located on the horizontal axis, and the area under the curve (AUC) is also used for classification. The best accuracy obtained belongs to the points located in the top left corner. The value of AUC is closer to one, the more accurate classification is occurred. According to the obtained results, the area under the curve for IR is 0.95 which is close to 1, indicates that the prediction ability of this model is 95%. After IR, KNN with accuracy of 92% stands in the second place and DT hast the lowest AUC which means that this model is not capable as IR and KNN when it is evaluated by ROC curve.

C. Class Prediction Error

Class prediction error provide a bar plot in which the horizontal axis is the actual class and the vertical is the number of predicted class's instances. The proportion of instances predict truly against those predicted incorrectly can be visualized by this plot and the application of it is similar to the confusion matrix. As an example, the class prediction error for Logistic Regression classifier is provided in Fig. (10). In this plot if you divide the first bar into twelve cells each one represents 10 instances. Indeed one can imagine the 11 out of 12 instances that belong to the class 0 is predicted correctly. So, the corresponding accuracy of first type (class 0) in this case would be approximately 91%. Another way, you can attribute the approximated number to the boundaries of this bar and again calculate the accuracy, So, in the first glance one can estimate that the model is of great accuracy or not.

D. Ridge Classifier

Ridge classifier confusion matrix indicates that the number of 10 instances which belong to the class 0 misclassified as class 1 and 117 instance classified correctly as class 0. Similarly, although 94 instances which belong to class 1 classified correctly, 23 instances which belong to this class misclassified as class 0.

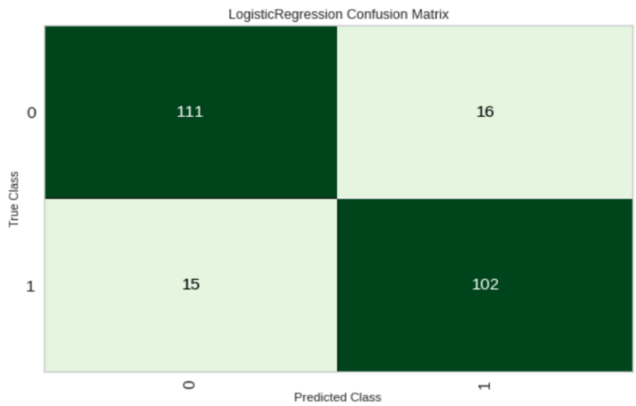

Fig. 10. Class prediction error for Logistic Regression

From confusion matrix the accuracy of Ridge classifier has been estimated to be 87% which is remarkable and fair. Class prediction error bar chart indicates that almost 120 instances out of 140 are classified correctly as class 0 and 20 instances of this class misclassified as class 1, suggesting that the classification accuracy of class 0 for ridge classifier is equal to 86% (divide 120 by 140 or 6/7). Similarly, for class 1 prediction, almost 90 instances out of 100 predicted correctly as class 1 and the accuracy of Ridge classifier for classification of class 1 is estimated to be 90% which is considerable.

E. Results Comparison

This section compares the proposed approach's results with linear MMLDF, fragmented MMLDF, and simple SVM methods on the UCI benchmark dataset. The accuracy obtained for different methods is compared in Table

(6). Using the introduced approach, the better accuracy can be achieved.

Table 6. Comparison of accuracy in different methods

Method	Bupa	Iris	Madelon
MMLDF	68.28	73.33	58.22
Normal SVM	70.28	97.33	59.31
MMLDF piece-wise	72.85	98.00	61.21
Proposed method	74.29	98.03	80.39

VIII. CONCLUSION

In this study, by integrating DHT22 sensors with the Esp32 microcontroller, we were able to collect accurate data on humidity and temperature in the mushroom cultivation environment. Then, the collected data was sent to the Blynk mobile application, enabling users to remotely monitor the conditions and make informed decisions. Additionally, the system incorporated relays connected to a fog machine and an air conditioner for humidity and temperature control, respectively. Furthermore, the system was powered by a solar power system, making it energy-efficient and environmentally friendly. In this project, the data generated by the analysis of the images taken has been used. Since the data set has a very large volume, it is necessary to perform pre-processing on them to implement practical purposes. So, a hybrid technique was employed to select the optimal features of images. The approach aimed to strike a balance between efficiency and accuracy by optimizing a given criterion that characterizes the subset of features and the associated selected instances. The choice of the differential evolution algorithm was motivated by its ability to converge effectively and identify standard features among the objects in the images using a limited number of features. This algorithm utilizes selection, mutation, and crossover operators to iteratively improve the conditions over multiple generations. Despite its simplicity and low computational complexity, the differential evolution method can deliver high-performance quality in machine learning.

At first step, features were extracted from the data that show the degree of their interaction with each other. Then these features have been evaluated by methods such as logistic regression, k-nearest neighborhood and decision tree. The objective function used in this project is a multi purpose function that simultaneously focuses on minimizing the number of selected features and redundancy features. In this situation, it was found that among the specified features, the first two features covered more than 89% of the variance of the entire collection, which was also confirmed by drawing two charts, Scree plot and Pareto plot. Then the wavelet transform method is applied to two main features and it is stated that by reducing the number of features to 2, a considerable amount of calculations is reduced and only about 4% of the accuracy provided for the estimated results is reduced. To achieve these results, 90 models of measured data were used, 81 samples for model design and 9 samples It has been used to measure the accuracy of the estimate. In conclusion, the integration of IoT Blynk, along with the DHT22 sensor, relays, and solar power system, has demonstrated the potential to revolutionize mushroom cultivation. This study opens up new possibilities for precision agriculture and smart farming practices, paving the way for improved yields and sustainable mushroom production. Among the advantages of the mentioned approach, we can mention the extraction of effective features with the help of using a hybrid approach including DEA and WT. In order to classify the extracted features, several methods such as RL, K-NN and DT methods have been used, which their quality of performance have been evaluated by various criteria, including ROC and F1-score. The accuracy obtained in the results shows that by using the proposed combined method, appropriate evaluations can be implemented on the received images.

REFERENCES

[1] G. Jayavardhana, R. Buyya, S. Marusic, and M. Palaniswami, "Internet of Things (IoT): A vision, architectural elements, and future directions", *Future generation computer systems*, vol. 29, no. 7, 2013, pp. 1645-1660.

[2] H. LiBo, X. Chai, Z. Lin, L. Tan, D. Qing, T. Lin, and L. Yang, "Preliminary study of modeling and simulation technology oriented to Neo-type artificial intelligent systems", *Journal of System Simulation*, vol. 30, no. 2, 2019, pp. 349-362.

[3] C. Deepak, and Latika Kharb, "Smart diagnosis of orthopaedic disorders using internet of things (IoT)", *International Journal of Engineering and Advanced Technology,* vol. 8, no. 6, 2019, pp 215-220.
[4] B. Hossain, and M. Islam. "Use of artificial intelligence for precision agriculture in Bangladesh." *Journal of Agricultural and Rural Research,* vol. 6, no. 2, 2022, pp. 81-96.
[5] J. M. Talavera *et al.,* "Review of IoT applications in agro-industrial and environmental fields", *Computers and Electronics in Agriculture,* vol. 142, 2017, pp. 283-297.
[6] P. Stamets, *growing gourmet and medicinal mushrooms*. Ten speed press, CA: Berekley, 2011, pp. 54-59.
[7] V.K. Chaturvedi, and P. Verma, *Handbook of mushrooms,* Aavishkar Publishers, Distributors, 2013.
[8] D. J. Royse, "Speciality mushrooms: Cultivation on synthetic substrates in the USA and Japan", *Interdisciplinary Science Reviews,* vol. 20, no. 3, 1995, pp. 205-214.
[9] P. G. Miles and S. Chang, *Mushroom biology: concise basics and current developments,* World Scientific, NJ: River Edge, 1997, pp. 62-64.
[10] Y. Li *et al.*, "Effects of light irradiation on the textural properties and energy metabolism of postharvest shiitake mushrooms (Lentinula edodes)", *Journal of Food Processing and Preservation,* vol. 45, no. 12, 2021. DOI: 10.1111/jfpp.16066.
[11] Q. Wang *et al*., "Impact of various cultivation substrates on the medicinal properties of reishi mushrooms (Ganoderma lucidum)", In *Proc. of the International Symposium on Mushroom Cultivation and Mycology,* 2020, pp. 45-50.
[12] S. Patel *et al.,* "Utilization of agricultural waste as substrates for oyster mushroom cultivation", In *Proc. of the International Conference on Sustainable Agriculture and Environmental Sciences*, pp. 234-239, 2018.
[13] Binti Sulaiman, N.A., Bin Sadli, N.D.D.: "An IoT-based smart garden with weather station system", *In Advances in Smart Communication Technology and Information,* 2019, pp. 205-212. DOI: 10.1007/978-3-030-22088-2.
[14] Susmitha, P., Bala, G.S, "Design and implementation of a smart home automation system using Blynk", In *Proc. 2018 International Conference on Recent Trends in Information Technology (ICRTIT)*, pp. 1-6, 2018. DOI: 10.1109/ICRTIT.2018.8403800.
[15] J.H. Holland, "Genetic algorithms." *Scientific American,* Vol. 267, no. 1, 1992, pp. 66-73.
[16] I. Rechenberg, "Evolutionsstrategien", *Simulationsmethoden in der Medizin und Biologie*, 1978, pp. 83-114.
[17] R. Storn, and K. Price, "Differential evolution–a simple and efficient heuristic for global optimization over continuous spaces", *Journal of global optimization,* vol. 11, no. 4, 1997, pp. 341-359.
[18] J. Kennedy, and R. Eberhart, "Particle swarm optimization", In *Proc. of ICNN 95-international conference on neural networks,* vol. 4, 1995, pp. 1942-1948.
[19] M. Dorigo, V. Maniezzo, and A. Colorni, "Ant system: optimization by a colony of cooperating agents", *IEEE Transactions on Systems, Man, and Cybernetics, Part B (Cybernetics),* vol. 26, no. 1, 1996, pp. 29-41.
[20] D. Karaboga, *An idea based on honey bee swarm for numerical optimization,* Vol. 200, Technical report-tr06, Erciyes university, engineering faculty, computer engineering department, 2005.
[21] I. Oh, J. Lee, and B. Moon. "Hybrid genetic algorithms for feature selection." *IEEE Transactions on pattern analysis and machine intelligence*, vol. 26, no. 11, 2004, pp. 1424-1437.
[22] S. Gu, R. Cheng, and Y. Jin, "Feature selection for high-dimensional classification using a competitive swarm optimizer", *Soft Computing,* vol. 22, no. 3, 2018, pp. 811-822.
[23] A. Onan, and S. Korukoğlu, "A feature selection model based on genetic rank aggregation for text sentiment classification", *Journal of Information Science,* vol. 43, no. 1, 2017, pp. 25-38.
[24] E. Emary, H. M. Zawbaa, and A. E. Hassanien, "Binary grey wolf optimization approaches for feature selection", *Neurocomputing,* vol. 172, 2016, pp. 371-381.
[25] B. Mohseni Bababdani, and M. Mousavi. "Gravitational search algorithm: A new feature selection method for QSAR study of anticancer potency of imidazo [4, 5-b] pyridine derivatives", *Chemometrics and Intelligent Laboratory Systems,* vol. 122, 2013, pp. 1-11. DOI: 10.1016/J.CHEMOLAB.2012.12.002.
[26] X. Han *et al*., "Feature subset selection by gravitational search algorithm optimization", *Information Sciences,* vol. 281, 2014, pp: 128-146.
[27] M. Bardamova, A. Konev, I. Hodashinsky, and A. Shelupanov, "A fuzzy classifier with feature selection based on the gravitational search algorithm", *Symmetry,* vol. 10, no. 11, 2018, pp. 609. DOI:10.3390/sym10110609.
[28] R. Guha, M. Ghosh, A. Chakrabarti, R. Sarkar, and S. Mirjalili, "Introducing clustering based population in binary gravitational search algorithm for feature selection", *Applied Soft Computing,* vol. 93, 2020. DOI: 10.1016/j.asoc.2020.106341.
[29] D. Rodrigues *et al*., "Optimizing feature selection through binary charged system search", *International Conference on Computer Analysis of Images and Patterns,* 2013, pp. 377-384.
[30] E. Pashaei, and N. Aydin, "Binary black hole algorithm for feature selection and classification on biological data", *Applied Soft Computing,* vol. 56, 2017, pp. 94-106. DOI: 10.1016/j.asoc.2017.03.002.

[31] O. S. Qasim, N. A. Al-Thanoon, and Z. Y. Algamal, "Feature selection based on chaotic binary black hole algorithm for data classification", *Chemometrics and Intelligent Laboratory Systems,* vol. 204, 2020, pp. DOI: 10.1016/j.chemolab.2020.104104.

[32] N. Dif, and Z. Elberrichi, "Microarray data feature selection and classification using an enhanced multi-verse optimizer and support vector machine", *3rd international conference on networking and advanced systems,* 2017.

[33] W. Cai, X. Wen, and Q. Tu, "Designing an intelligent greenhouse monitoring system based on the Internet of Things", *Applied Ecology & Environmental Research,* vol. 17, no. 4, 2019.

[34] A. Aher, J. Kasar, P. Ahuja, and V. Jadhav, "Smart agriculture using clustering and IOT", *International Research Journal of Engineering and Technology (IRJET),* vol. 5, no. 03, 2018, pp. 4065-4068.

[35] A. Maier, A. Sharp, and Y. Vagapov, "Comparative analysis and practical implementation of the ESP32 microcontroller module for the internet of things", *2017 Internet Technologies and Applications (ITA)*, 2017, pp. 143-148. DOI: 10.1109/ITECHA.2017.8101926.

[36] A. Debnath, A. Ghosh and D. Mandal, "Smart Greenhouse Monitoring and Controlling System Using IOT", *2019 3rd International Conference on Trends in Electronics and Informatics (ICOEI)*, 2019, pp. 416-420.

[37] L. Fan *et al.*, "Optimal Control of Solar Inverter for Power Management in Grid-Tied Microgrids", *IEEE Transactions on Power Electronics*, vol. 29, no. 8, , 2014, pp. 4369-4381.

[38] D.D Lewis, Y. Yang, T. G. Rose, and F. Li, “Rcv1: A new benchmark collection for text categorization research”, *Journal of machine learning research*, vol, 5, 2004, pp. 361-397.

[39] https://sentinel.esa.int/web/sentinel/missions/sentinel-2

[40] T. Kuchkorov, S. Urmanov, M. Kuvvatova, and I. Anvarov, “Satellite image formation and preprocessing methods”, *2020 International Conference on Information Science and Communications Technologies (ICISCT),* 2020, pp. 1-4.

[41] Q. Yuanwei *et al*., “Mapping paddy rice planting area in cold temperate climate region through analysis of time series Landsat 8 (OLI), Landsat 7 (ETM+) and MODIS imagery”, *ISPRS Journal of Photogrammetry and Remote Sensing,* vol. 105, 2015, pp. 220-233.

[42] F. Rahmani, C. Valmohammadi, and K. Fathi, "Detecting fraudulent transactions in banking cards using scale-free graphs", *Concurrency and Computation: Practice and Experience*, vol. 34, no. 19, 2022. DOI: 10.1002/cpe.7028.

[43] C. Valmohammadi, and F. Rahmani, "A hierarchal model of coding knowledge towards facilitating knowledge transfer in organizations", *Information Discovery and Delivery*, vol. 50, no. 2, pp. 155-164, 2022. DOI: 10.1108/IDD-08-2020-0105.

[44] A. Alhammadi *et al*.," Prediction of Environmental Conditions of the Greenhouse Using Neural Networks Optimized with the Grasshopper Optimization Algorithm (GOA)", *Journal of Power System Technology*, vol. 48, no. 3, pp. 622-635, 2024.